PalArch's Journal of Archaeology of Egypt / Egyptology

IMPROVING THE AERODYNAMIC PERFORMANCE OF THE BLADE OF 3D WIND TURBINE BY DESIGNING THE BLADE GEOMETRY

Alireza SHirzadegan[1] , Reza Aghaei togh[2], Fereidoon Sabetghadam[3]*

[1] Phd Student, aerospace engineering, Islamic Azad university science and research branch, engineering faculty, Tehran, Iran (Email: alireza.shirzadegan@srbiau.ac.ir).

[2]Associate Professor, aerospace engineering, engineering faculty, Islamic Azad university science and research branch, Tehran, Iran(Corresponding Author)* (Email: reza_tog@srbiau.ac.ir).

[3]Associate Professor, aerospace engineering, engineering faculty, Islamic Azad university science and research branch, Tehran, Iran (fsabet@srbiau.ac.ir).

Alireza SHirzadegan , Reza Aghaei togh, Fereidoon Sabetghadam: Improving the aerodynamic performance of the blade of 3D wind turbine by designing the blade geometry-- Palarch's Journal Of Archaeology Of Egypt/Egyptology 18(7), ISSN 1567-214x

Keywords: Renewable Energy, Wind Turbine, Swallow Blade, Seagull Blade, Optimization.

ABSTRACT

The purpose of the study was to present new geometries of wind turbine blades based on natural patterns (like birds) so that the aerodynamic efficiency (ratio of lift to drag coefficient) and optimal pressure coefficient can be obtained. In the next step, the new blades introduced in the present study called swallow geometry blades and seagull geometry blades were modeled and their performance was evaluated and compared with the base blade. This was done numerically in CFX software in two Reynolds numbers 60,000 and 80,000 and at angles of attack from 0 to 20 degrees. According to the studies conducted and the results obtained from the graphs about the condition of the lift, drag and pressure ratios, one can state that the blade with swallow geometry and the blade with seagull geometry can be a good alternative to the blade with NACA 23012 geometry. As a result, it can be said that by replacing these two blades in the construction of 3-blade horizontal axis wind turbines, with small and medium size, a much higher power factor and efficiency can be achieved which can be a big change in the construction of horizontal axis wind turbines with small and medium size.

1. INTRODUCTION

Nowadays, everyone knows the necessity of replacing fossil fuels. Some countries without fossil fuel resources have a higher incentive to replace fossil fuels with resources and have been more pioneering than others. Overall, one can reduce greenhouse gas emissions by replacing wind energy with wind power from fossil fuel power plants. On the other hand, the natural attractions and landscapes of wind energy systems are considered a symbol of clean energy for people [1]. Moreover, 99% of the

land allocated for wind farm construction can be used for agricultural and livestock activities and only about 1% is used by turbines. Power generation forms only one part of a country's energy. Thus, wind force alleviates the negative effects. As wind can replace fuel for electricity generation, wind power can reduce global warming. Moreover, unlike fossil or nuclear power plants that use large volumes of water to cool facilities, wind turbines do not need water to generate electricity. At the moment, the largest capacity of installed wind turbines in recent decades has been the on-grid type. However, sometimes off-grid wind turbines are used in remote areas too. Most wind turbines start generating electricity when the wind velocity is about 3 to 4 meters per second, producing a maximum allowable power of about 15 meters per second [2]. Nowadays, many wind turbines have been installed and operated. These turbines have been produced in various generations and completed over time. Wind power generation capacity quadrupled from 2000 to 2006. One can state that wind power generation doubles every three years. In countries like Denmark and Spain, as forerunners regarding this, more than 10% of their electricity is generated by wind, and about 81% of wind turbines are installed in the United States and Europe [3].

Given the wind changes, there is limited predictability for the output of wind farms. Wind must be programmable like other sources of energy. However, the nature of the wind changes this phenomenon inherently. Although some approaches are used to predict the power generation of these power plants, the predictability of these power plants is overall low. These problems of power plants are usually partially eliminated by using energy storage approaches like using pumped water power plants. Wind resources are wind farm fuel, and small changes effect a major effects on its commercial value. Thus, even small changes in average wind velocity can make a big difference in efficiency. Some information obtained from studying the wind technology market in Germany as a leader in the world wind industry shows the trends in recent years in this industry, attention to which will be useful in predicting the future. The average capacity of wind turbines installed in Germany is about 1000 kWh. However, if we consider only the turbines installed in the first half of 2007, the average capacity of new wind turbines is about twice this value. Hence, a clear trend of increasing the size of modern wind turbines is observed [4].

A paper entitled “Optimization of wind turbine blades” in MIT University in April 2010 studied and analyzed the geometric shape of the turbine blade, the control screw method and wind velocity changes [5]. This method has been designed and tested for a right angle arrangement. Using genetic algorithm (GA), they have tried to maximize the output energy while minimizing the blade volume and destructive pressures on it. Based on the results from DOE and SQP software in this study, the efficiency obtained is between 60 and 70% of the efficiency of Betz's law at the best points.

In a paper entitled “Examining the effect of turbulence using computational fluid dynamics on the aerodynamics of horizontal wind turbines” in July 2011 in Amirkabir University, Mansour and Yahyazadeh modeled aerodynamics of horizontal wind turbines numerically using CFD in three various turbulence models [6]. The obtained turbulence modeling

results have a very high degree of reliability. The blades are located at a screw angle of 12° and the results for various turbulence modes are recorded according to RNG K-ε and SPALART-ALLMARAS standards and compared with experimental data from the National Renewable Energy Laboratory (NREL) for two various velocities. Finally, the study indicated that the CFD calculations for the aerodynamics of horizontal axle-based wind turbine blades based on RNG K-ε for low velocities are more consistent with the experimental data and the SPALART-ALLMARAS model for high velocities is more consistent with the experimental data.

In another paper entitled "WAKE shock analysis in the turbulence layers behind the wind turbine," Fort and Porte (December 2011) examined the shock behind the wind turbines and obtained the closest shock in the turbine layers behind the turbine flow. Moreover, they have shown these shocks in some figures (extracted from fluent software) based on the distance in the direction of wind flow and perpendicular to the wind flow behind the turbine. In other figures by keeping constant the distance in the direction of the wind flow, they change the distance in the direction perpendicular to the flow in both Y and Z directions, and finally identify the worst states at various distances, suggesting that much better the efficiency will be attained if the shock effects from turbulence layers reduce [7].

Given the study of the practical and theoretical studies on wind turbines and wind energy, one can clearly state that the main topics of the day for wind turbines is to increase the efficiency of wind turbines and how to delay the separation in the flow and improve lift and drag ratios. Researchers have done a lot of work Regarding this like examining the distance of turbulent flow to the wind turbine blade, using methods like plasma to delay separation, examining flexible blades and elasticity, analyzing wind turbines in unstable flows, and studying turbulent flow behavior with a wake behind the wind turbine blades, examining the oscillations and vibrations in the wind turbine blades and using tools like vortex generator to delay separation and many other things. However, what has received more attention in recent years to improve the operating efficiency of wind turbines has been the change in the geometry of wind turbine blades. This is because this approach gives better and more effective results in enhancing the performance of wind turbines. Regarding this, the idea of wind turbine blades has been taken from the same change and 2 blades modeled and studied with geometry taken from nature in the present study.

2. METHODS

2.1. Selecting the base wind turbine for windy sites

2.1.1. Wind turbine specifications

Various environmental conditions affect wind turbines, so that these conditions have a significant role in the output load and useful life and operation of turbines. All environmental and soil parameters must be considered in reaching greater reliability and higher safety factor for the optimal choice of turbine type.

The environmental conditions are divided into two subsets: normal winds and high winds. Normal wind conditions have a long-term effect on

the loads on the structure and operating conditions, whereas high winds, although rare, can potentially cause critical conditions. Wind turbines are grouped into various classes according to their tolerance and capacity against wind conditions based on IEC 61400-1 Rev2.

These classes are categorized according to the average wind velocity over a ten-minute period, with the probability of stronger winds occurring once every 50 years, and the average annual wind velocity at the height of the turbine.

Table 1: The class of wind turbines according to IEC standard

WT classes	**I**	**II**	**III**	**IV**
V_{ref} [m/s]	50.0	42.5	37.5	30.0
V_{ave} [m/s]	10.0	8.5	7.5	6.0
A $_{I15}$	0.18	0.18	0.18	0.18
B $_{I15}$	0.16	0.16	0.16	0.16

The numbers shown in Table 1 are the maximum values for each wind class

V_{ref}: 50-year average wind velocity over a period of 10 minutes

V_{av}: Average annual wind velocity at hub altitude

A: Determiner of subgroup for high wind characteristics and severe turbulence

B: Determiner of subgroup for high wind characteristics and weak disturbances

L_{15}: Characteristic value of turbulence intensity at a velocity of 15 meters per second

2.1.2. Strong winds

Turbines have to be designed to withstand high winds. High wind conditions can be classified according to the maximum average wind velocity obtained in a given period. According to the IEC standard, reversible periods are set over a period of 50 years, and the base wind velocity (V_{ref}) is the average wind velocity every ten minutes over a period of 50 years. V_{ref} parameter is specified according to the anemometer operations performed on the site (area) in Wind Pro software.

2.1.3. Average annual wind velocity

The average annual wind velocity for hub heights (V_{av}) is obtained using various meteorological software and anemometer operations.

Overall, besides suitable environmental conditions, other side factors lie wind continuity, calculation of wind density, site access conditions (windy area), traffic restrictions, being earthquake prone, soil science, urography (ground and elevation) and even the surface and ground roughness conditions where the wind turbine is to be installed should also be considered to select and install a wind turbine. This is because if the surface roughness is high, it can lead to turbulent flow and damage to the wind turbine blade structure and reduce the wind turbine output power.

2.1.4. Determining the base wind turbine class

Then based on inquiries from Renewable Energy and Energy Efficiency Organization and wind turbine manufacturers, the famous geometries used in wind turbine blades are NACA4412, NACA4415, NACA4418, NACA23012, NACA23015, and NACA23018. In the next step, these blades are modeled and analyzed to determine which one has the lowest drag-to-lift ratio (Cd / Cl). This analysis was done at attack angles from 0 to 20 degrees.

Table 2: Drag-to-lift ratio at various angles for the blades

Attack angle	Lift ratio	Drag ratio	Drag-to-lift ratio
Airfoil 4412			
0	0.779	0.0118	0.015107845
2	0.886	0.0125	0.014108352
3	0.985	0.0134	0.013904061
4	1.074	0.0145	0.013800931
5	1.154	0.0163	0.014124783
6	1.225	0.019	0.015510204
7	1.288	0.021	0.016304348
8	1.341	0.0228	0.017002237
9	1.386	0.0254	0.018326118
10	1.423	0.0278	0.019536191
11	1.451	0.0304	0.020951068
12	1.47	0.0333	0.022653061
13	1.482	0.038	0.025641026
14	1.484	0.0418	0.028167116
15	1.478	0.0459	0.03105548
16	1.463	0.054	0.036910458
17	1.438	0.0552	0.038386648

18	1.403	0.0602	0.042908054
19	1.358	0.0665	0.048969072
20	1.323	0.0674	0.051325790
Airfoil 4415			
0	0.273	0.0125	0.045787546
1	0.395	0.0123	0.031139241
2	0.517	0.0125	0.02417795
3	0.639	0.013	0.020344288
4	0.761	0.0136	0.017871222
5	0.874	0.0148	0.016933638
6	0.971	0.0162	0.016683831
7	1.056	0.0175	0.01657197
8	1.13	0.0191	0.016902655
9	1.193	0.021	0.017602682
10	1.245	0.0288	0.02313253
11	1.286	0.0247	0.019206843
12	1.317	0.0278	0.02110858
13	1.338	0.033	0.024663677
14	1.349	0.033	0.024462565
15	1.35	0.0359	0.026592593
16	1.341	0.0391	0.029157345
17	1.322	0.0424	0.032072617
18	1.292	0.0458	0.035448916
19	1.251	0.0528	0.042206235
20	1.199	0.0573	0.047789825

Airfoil 4418			
0	0.562	0.0135	0.024021352
1	0.686	0.0136	0.019825073
2	0.8	0.014	0.0175
3	0.88	0.0139	0.015795455
4	0.952	0.0148	0.015546218
5	1.016	0.0158	0.015551181
6	1.073	0.0163	0.015191053
7	1.122	0.0177	0.015775401
8	1.165	0.02	0.017167382
9	1.201	0.0219	0.018234804
10	1.23	0.0241	0.019593496
11	1.253	0.0266	0.02122905
12	1.269	0.0285	0.022458629
13	1.28	0.0317	0.024765625
14	1.285	0.0342	0.026614786
15	1.283	0.0368	0.028682775
16	1.276	0.0396	0.031034483
17	1.263	0.0426	0.033729216
18	1.244	0.048	0.038585209
19	1.219	0.0516	0.042329779
20	1.188	0.0555	0.046717172
Airfoil 23012			
0	0.1266	0.0235	0.185624013
2	0.325	0.0138	0.042461538

4	0.5177	0.0066	0.012748696
6	0.697	0.036	0.051649928
8	0.859	0.07228	0.084144354
10	0.956	0.0111	0.011644578
12	1.098	0.0146	0.013096903
14	1.131	0.0164	0.014500442
16	1.0902	0.0147	0.013483764
18	1.022	0.1135	0.111056751
20	1.015	0.096	0.094581281
Airfoil 23015			
0	0.128	0.00087	0.04218744
2	0.223	0.00251	0.04792130
4	0.313	0.00143	0.058146965
6	0.5	0.0182	0.06860104
8	0.8427	0.06735	0.07992168
10	0.979	0.106	0.108273749
12	1.0977	0.149	0.135738362
14	1.172	0.1832	0.156313993
16	1.178	0.1923	0.163242784
18	1.145	0.1797	0.156943231
20	1.105	0.155	0.140271493
Airfoil 23018			
0	0.102	0.0152	0.09780245
2	0.299	0.0231	0.077257525
4	0.475	0.0309	0.010315789

6	0.652	0.0238	0.036503067
8	0.813	0.0597	0.073431734
10	0.957	0.1	0.104493208
12	1.0715	0.142	0.132524498
14	1.151	0.178	0.154648132
16	1.2	0.205	0.170833333
18	1.193	0.209	0.1751886
20	1.162	0.194	0.166953528

Based on the numbers obtained in Table 1, related to the lift and drag ratios of these blades, one can conclude that the blade with NACA 23012 geometry has the lowest lift ratio compared to the drag, among the most widely used blades, and therefore this blade can be selected as the best model used in the wind turbine blade or in other words as the base blade. In the following, the new blades introduced in the present proposal, called swallow blade and seagull blade, are modeled and their performance is evaluated and compared with the base blade.

2.1.5. Simulation of blades

With the geometric feature obtained, this blade is modeled in 3D and then meshed.

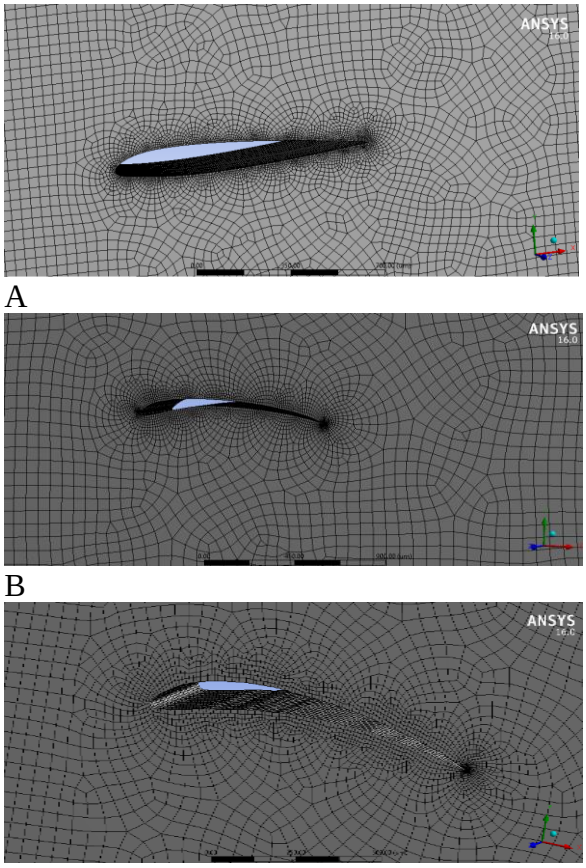

Figure 1: a) Blade mesh with NACA 2301 geometry, b) Blade mesh with SWALLOW geometry, c) Blade mesh with SEAGULL geometry

2.1.6. Governing equations

To solve any flow, it is necessary to solve the continuity and momentum equations to obtain the velocity components in the three directions of the coordinate axes. Now, if the flow is compressible or the physics of the problem involves multiphase flows, or if the study of heat transfer in the problem is considered, it is necessary to solve the energy equations along with the above set of equations.

2.1.6.1. Continuity equation

The equation of conservation of mass or continuity for smooth flow in the general case and in vector form is written as follows.

$$\frac{\partial \rho}{\partial t} + \nabla \cdot (\rho \vec{v}) = S_m \quad (1)$$

This equation holds for both compressible and incompressible flows. The term S_m represents the mass added to the continuous phase due to the change of state of the second phase in multiphase flows (like evaporation of liquid droplets and their addition to the gas phase).

2.6.1.2. Momentum equations

Momentum equations are written in an inertial coordinate system (origin of non-acceleration coordinates) for smooth flow as follows:

$$\frac{\partial \rho}{\partial t}(\rho \vec{v}) = \nabla \cdot (\rho \vec{v} \vec{v}) = -\nabla p + \nabla \cdot (\vec{\tau}) + \vec{F} \quad (2)$$

In the above phrase, p is the static pressure and $\vec{F}$ the volumetric forces applied on the fluid, such as the force of gravity or the forces acting on the liquid phase or phases **b**ecause of the interaction in a multiphase flow.

2.1.7. Flow solution method

Here, the solution of the equations governing the fluid flow is done in CFX software. The convection terms in the momentum equations are discretized using the second-order upstream method, and the velocity and pressure correction is done using simple method. Flow disturbances are modeled using the SST-Kω model, which is one of the turbulence models in engineering and has a higher capability than other models. A non-slip boundary condition is used for the blade wall. The geometry is selected in 3D, stable flow and ideal gas. Moreover, all the analyses were done at an attack angle between 0 and 20 degrees and at Reynolds numbers 60,000 and 80,000.

3. RESULTS

3.1. The results for blades with NACA 23012 geometry

A velocity and pressure contour and a relative velocity vector have been plotted to examine the flow around this wing in more detail. These 3 contours are plotted at the attack angle zero as is seen. According to the velocity contour, one can see that there is the highest velocity at the attack edge and as one move towards the escape edge, the velocity decreases and the pressure increases. The pressure contour for this airfoil indicates that the pressure at the top and bottom of the blade do not differ much and one cannot expect a very high lift coefficient in this blade (Figure 2a).

The results for the blade with SWALLOW geometry: The velocity and pressure contour and the relative velocity vector have been plotted to study the flow around this blade in more detail. According to the images below, these 3 contours are plotted at attack zero angle as is seen. According to the velocity contour, one can see that the highest velocity is at the attack edge, and the velocity decreases and the pressure increases as one move towards the escape edge. However, looking at the pressure contour,

one can see that the lower part of the blade has more pressure than the top of the blade, and this difference is felt and we can expect to have more lift in this geometry compared to the previous wing pressure contour (NACA 23012) (Figure 2b).

The results for the blade with SEAGULL geometry: A velocity and pressure contour has been plotted to examine the flow around this blade in more detail. According to the figures below, these 3 contours are plotted at the zero attack angles. Given the velocity contour, one can see that there is the highest velocity at the attack edge and the velocity decreases and the pressure increases as we move towards the escape edge. However, looking at the pressure contour, one can see that the lower part of the blade has more pressure than the top of the blade, and compared to the blade pressure contour (NACA 23012) this difference is felt and it can be expected that this geometry has a higher coefficient than the NACA 23012 wing (Figure 2 c).

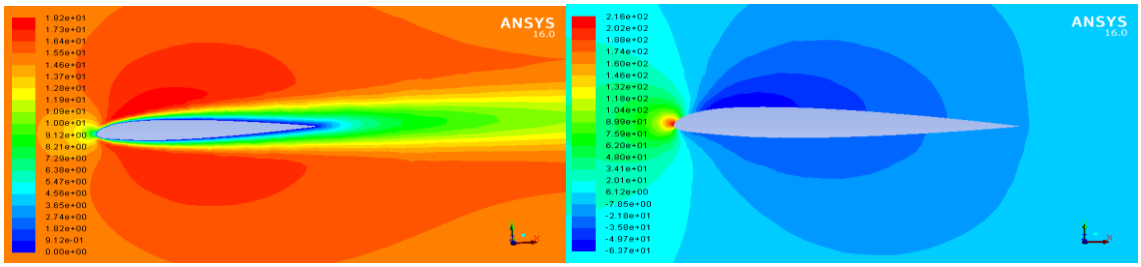

A

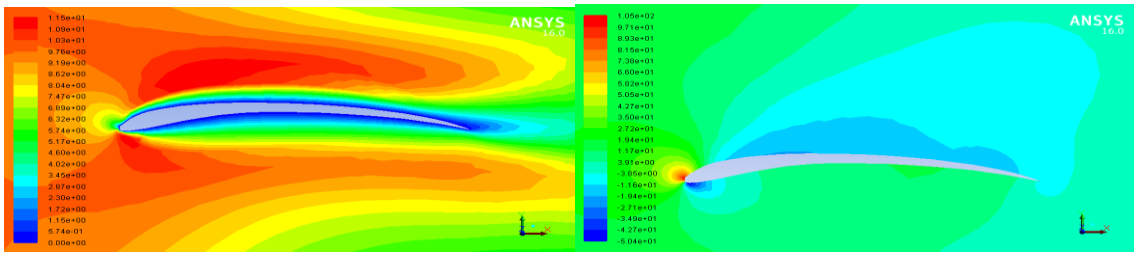

B

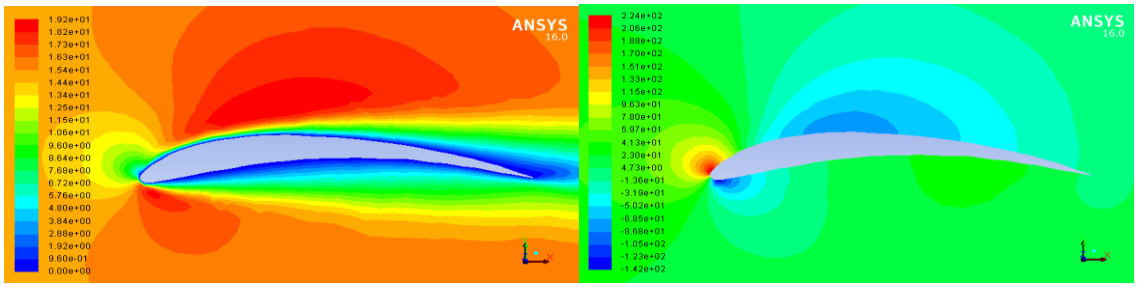

C

Figure 2: a) Velocity contours for blade with NACA 23012 geometry, pressure contour for blade with NACA 23012 geometry

B) Velocity contour for blades with SWALLOW geometry, pressure contour for blades with SWALLOW geometry

C) Velocity contour for blade with SEAGULL geometry, pressure contour for blade with SEAGULL geometry

3.2. Examining the results

For more understanding, the ratios of drag, lift, lift to drag and the pressure ratio for these blades has been compared in a diagram. According to the drag ratio in the Reynolds number 60,000, one can see that the blade with NACA 23012 geometry starts from 0.01 in the zero attack angle and reaches about 0.04 in the attack angle of 20 degrees. If in the blade with swallow geometry, this coefficient starts from about 0.02 at the attack angle of zero and at the attack angle of 10 degrees, the drag ratio reaches 0.04, but then from the attack angle of 10 to 20 degrees, this ratio increases more and reaches about 0.22. In the seagull blade, the drag ratio starts at 0.02 at the zero attack angle and ends at 0.13 at the angle of 20 degrees. This applies to the Reynolds number 80,000, except that the drag ratio for each of the 3 blades decreases from 0 to 20 from the attack angle because of less viscous

effects - Especially for wings with seagull geometry, the reduction in drag ratio is greater than the Reynolds number 80,000. According to these two diagrams, one can see that NACA 23012 blade has a better condition (has a lower drag ratio) than the swallow blade and the seagull blade and the seagull blade has a lower drag than the swallow blade. One has to note that the difference in drag ratio for the NACA 23012 blade is very small compared to the other two blades. Especially from the attack angle from 0 to 10 degrees, the difference between the two blades for NACA 23012 and the seagull wing at Reynolds number 60,000, about 0.01 and at Reynolds number 80,000, this difference is almost zero. Additionally, the difference between the two blades of NACA 23012 and the swallow wing in Reynolds number 60,000 is about 0.07 and in Reynolds number 80,000, this difference is less and reaches about 0.04. Overall, all 3 blades are in good condition in terms of drag ratio (Figure 3).

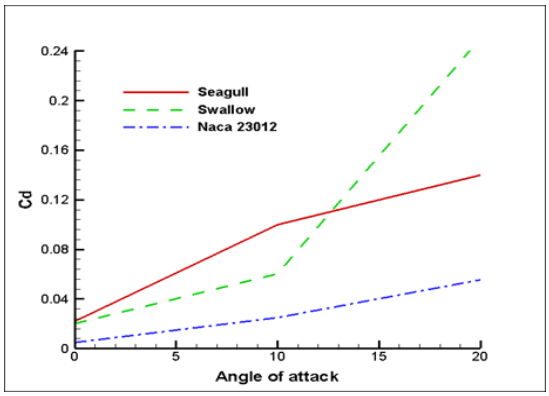

A

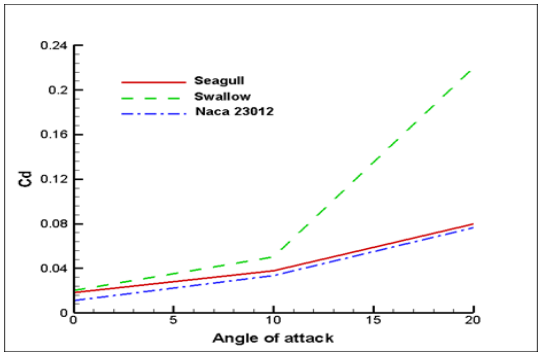

B

Figure 3: a) Comparison of the drag ratio of the three blades in terms of attack angle in the Reynolds number 60,000, b) Comparison of the drag ratio of the three blades in terms of attack angle in the Reynolds number 80,000

We will examine the lift ratio. According to the diagram, one can see that in Reynolds number 60,000, the lift factor for NACA 23012 blade starts from about 0.03 at an attack angle of 0, at an attack angle of 10 degrees it reaches 0.13 and then at an attack angle of 20 degrees it reaches 0.2. This is while the value of lift ratio for the seagull blade starts from 0.1 in the attack angle of 0 degrees and in the attack angle of 10 degrees reaches 0.8 and then in the attack angle of 20 degrees this ratio increases again and reaches 1.2. The value of the lift ratio for the swallow blade starts from about 1.1 in the attack angle of 0 degrees and reaches about 1.7 in the

attack angle of 10 degrees and then decreases slightly reaching 1.5 in the attack angle of 20 degrees. This happens with the Reynolds number 80,000 too. The difference is that the lift ratio for each of the 3 blades increases to some extent. The important point here is that unlike the drag ratio which was not much different for all 3 blades and all 3 blades with different geometries were in good condition in terms of drag ratio. Here, one can see that the lift ratio for 2 swallow blades and seagull is much better than the blade with the NACA 23012 geometry, especially for the swallow wing, which is in a better position compared to other blades. The state is very good and favorable compared to other blades especially in the attack angle of 0 to 10 degrees (Figure 4).

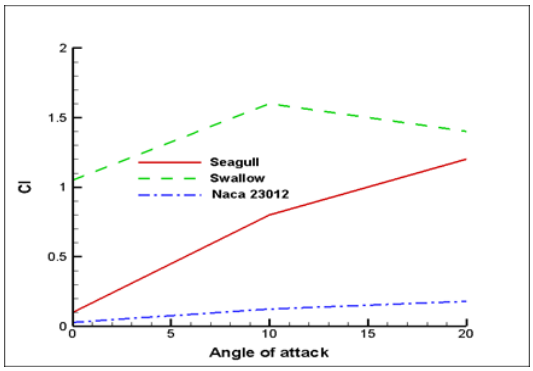

A

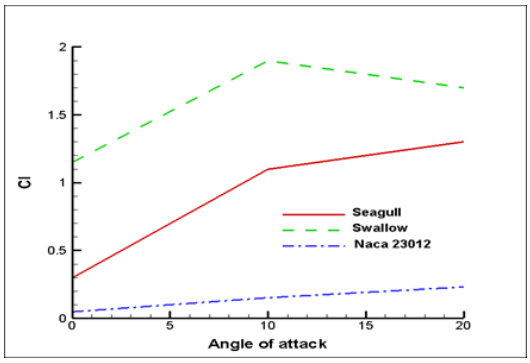

B

Figure 4: a) Comparison of the lift ratio of the three blades in terms of attack angle in the Reynolds number 60,000, b) Comparison of the lift ratio of the three blades in terms of attack angle in the Reynolds number 80,000

Now, we examine at the lift-to- drag coefficient in terms of attack angle. As Figure 5 shows, the value of this coefficient for the swallow blade at Reynolds number 60,000 and at an attack angle of 0 degrees, starts from about 58 and reaches about 40 at an attack angle of 10 degrees. However, it decreases from an attack angle of 10 to 20 degrees. It has a lot in this coefficient and reaches the value of about 10. For the seagull blade, this coefficient starts from 5 at the attack angle 0 and reaches about 9 at the attack angle of 10 degrees and then reaches 10 at the attack angle of 20 degrees. For NACA 23012 blade, it starts from 5 at the attack angle 0 and has a steady trend up to the attack angle of 10 degrees and remains in the range of 5, but from the attack angle of 10 to 20 degrees, this trend decreases and lift-to-drag coefficient decreases to 3. At the Reynolds number 80,000, the graph trend for the swallow blade does not change

much, from about 58 from the attack angle of 0 degrees starting at an attack angle of 20 degrees to about 10. However, in the seagull blade, the Reynolds number is 80,000 more, starting at 18 at an attack angle of 0 and reaching about 18 at an attack angle of 20 degrees. For NACA 23012, in Reynolds number 80,000, this coefficient is not much different and goes from 5 in the attack angle of 0 to 3 in the attack angle of 20. In this diagram, one can see that the drag coefficient for all 3 blades is not much different, yet the lift coefficient for the swallow blade is much higher in terms of attack angle for this blade as the lift-to-drag coefficient for the swallow blade is much higher than the other two blades.

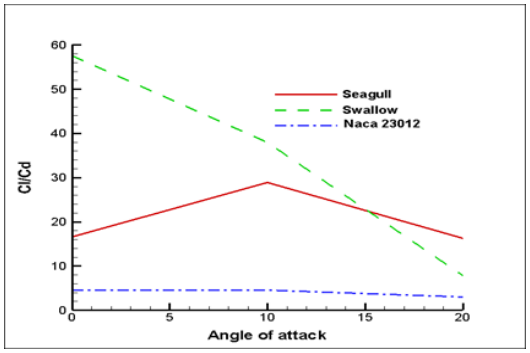

A

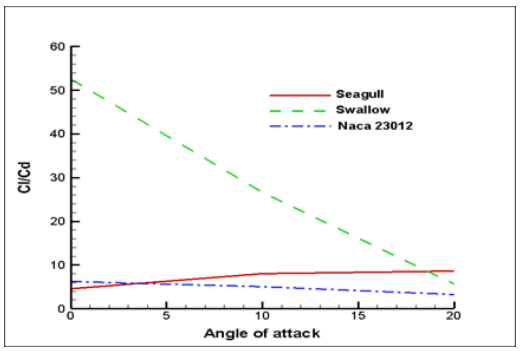

B

Figure 5: a) Comparison of lift-to-drag ratio of the three blades in terms of attack angle in the Reynolds number 60,000, b) Comparison of the lift-to-drag ratio of the three blades in terms of attack angle in the Reynolds number 80,000

Then the pressure coefficient for each of the 3 blades is compared. This comparison was made in 3 attack angles 0 and 20 and also in 2 Reynolds numbers 60,000 and 80,000 degrees. It has to be noted that this diagram shows the pressure difference between the surface and the bottom of the blade - the higher the pressure difference for each blade, the higher the blade. According to these diagrams, one can state that in Reynolds number 60,000, the largest pressure difference is related to the blade with swallow geometry at the attack angle of 0 degrees, and after the blade with seagull geometry, it has the highest pressure difference. As the attack angle increases, this pressure difference decreases for all 3 blades, but still, the blade with the swallow geometry has the largest pressure difference compared to the other blades, which means that the swallow blade has the highest lift coefficient. Looking at the pressure coefficient diagram in Reynolds number 80000, one can see that the swallow blade still has the

largest pressure difference in attack angles 0 and 20, followed by the seagull blade, except that the difference that in Reynolds number 80000 because of less viscosity, these pressure differences have generally increased.

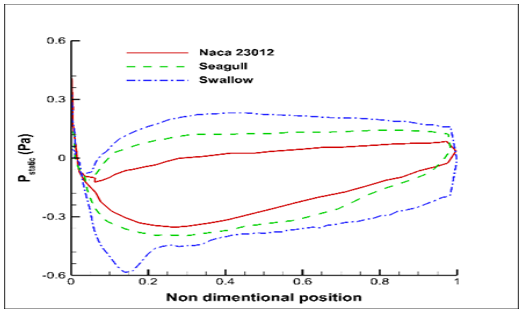

A

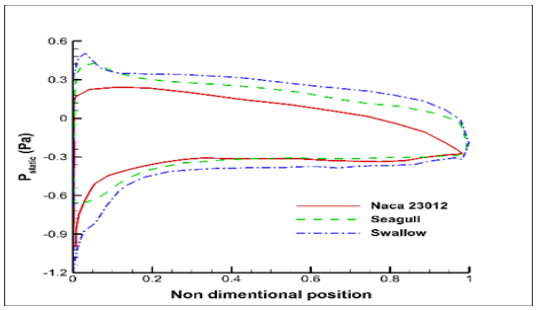

B

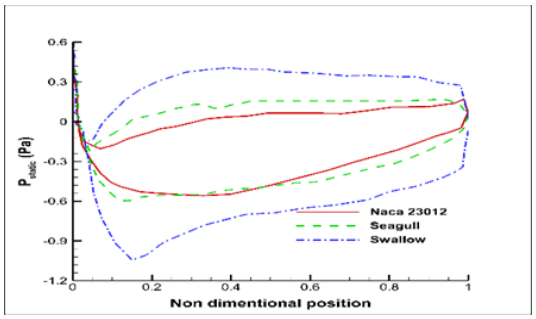

C

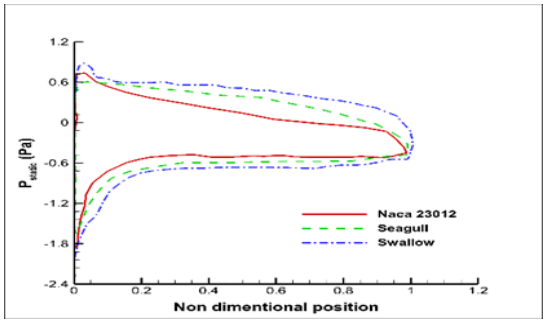

D

Figure 6: a) Comparison of the pressure coefficient of the three blades at attack angle 0 and in the Reynolds number 60,000, b) Comparison of the pressure coefficient of the three blades at attack angle 20 and in the Reynolds number 60000, c) Comparison of the pressure coefficient of the three blades at an attack angle of 0 and in the Reynolds number 80000, d) Comparison of the pressure coefficient for the three blades at an attack angle of 20 and the Reynolds number 80000

4. CONCLUSION

Given the survey of more than 25 years of practical and theoretical studies regarding wind turbines and wind energy, one can conclude that the main topics of the wind turbines are increasing the efficiency of wind turbines and how separation in the flow can be delayed and improvements can be made in lift and drag coefficients. The scholars have done many studies regarding this like examining the distance of turbulent flow to the wind turbine blade, using methods such as plasma to delay separation, examining flexible blades and elasticity, wind turbines analysis in unstable flows, and studying turbulent flow behavior and has a WAKE behind the wind turbine blades, examining the oscillations and vibrations in the wind turbine blades and using tools like vortex generator to delay separation and many other things. However, what has received more attention in recent years in improving the operating efficiency of wind turbines has been the change in the geometry of wind turbine blades, as this method produces better and more effective results in improving the performance of wind turbines. Regarding this, in the future study, the idea of the blade geometry change will be taken and 2 blades with geometry taken from nature modeled and studied. Regarding this, first, the best blade is selected by calculating the lift and drag coefficients (NACA 23012) among the blades widely used in wind turbines. Then the blade was modeled and examined in more detail and the velocity, pressure, relative velocity vector, lift coefficient and drag coefficient are obtained for this blade. Then the 2 other blades with swallow and seagull geometries were introduced and examined. The coefficients of lift, drag, velocity contour, pressure contour and relative velocity vector have been obtained for these two blades.

The blade with NACA 23012-geometry is one of the most famous and widely used blades used as a wind turbine blade with horizontal rotation axis and considered a blade with high performance. Then 2 blades with 2 different geometries were introduced that could be selected as a suitable alternative for NACA 23012 blade. According to the studies conducted and the results obtained from the above diagrams on the condition of the lift, drag and pressure coefficients, one can state that the blades with swallow and the seagull geometries can be a suitable alternative to the NACA 23012 blade. Thus, one can state that a much higher power factor and efficiency can be achieved by replacing these two blades in the construction of 3-blade wind turbines, small and medium size with horizontal axis, which could be a great change in the construction of small and medium wind turbines with horizontal axes.

5. VALIDATION

To validate the numerical results obtained from this research, the experimental NREL S826 [8] wind turbine was numerically modeled and then the turbine and its solution amplitude were networked and compared for both numerical and experimental states. As seen from Diagram 6, this wind turbine was numerically modeled and networked, and the pressure and torque coefficient diagram was numerically studied and compared with the experimental state. Looking at the pressure and torque coefficient diagrams, one would see that there is a good agreement between the two numerical

and experimental states, and the numerical work is said to enjoy an acceptable accuracy.

A

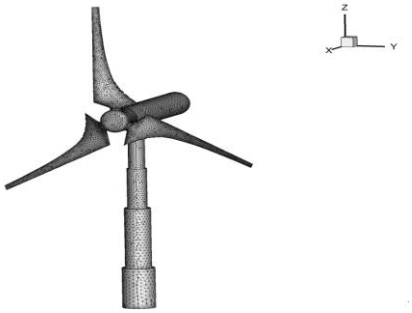

B

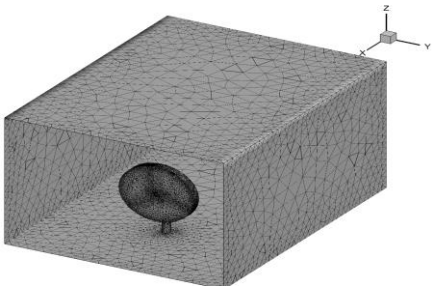

C

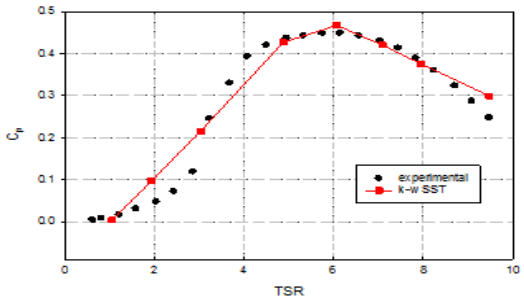

D

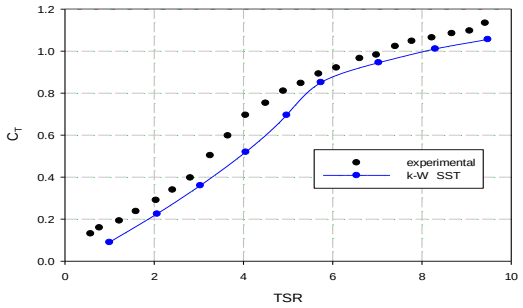

E

Figure 7: a) Experimental NREL S826 wind turbine; b) Numerically modeled NREL S826 wind turbine; c) Turbine networking and computational range for NREL S826 wind turbine d) Comparison of NREL S826 wind turbine pressure coefficient under two numerical and experimental states; e) Comparison of torque coefficient of NREL S826 wind turbine in both numerical and experimental states [8].

Acknowledgment: Hereby, I express my indebtedness to my dear professors. The research as supervised by these professors and the lessons learned from these great men led me to learn the research methods and teaching skills in addition to gaining valuable scientific themes. Also, my special gratitude goes to my dear parents who helped me complete my studies. I sincerely praise the role they have played in my life. I hope this research would make up a bit of their love and affection.

Nomenclature

R: Rotor radius (m)
V: Rotor velocity (m/s)
P: Wind turbine power (kW)
P: Wind density (kg/m^3)
A: Axial induction factor (no unit)
A: Blade's cross-section (m^2)
Q: Blade correction factor (no unit)
Ω: Torque coefficient (no unit)
β: Angle of attack (0̊)

REFERENCES

Ra.Cal, AN.Ramos, N.Hamilton, D.Houck,"Spacing dependence on wind turbine array boundary lay17th International Symposium on Applications of Laser Techniques to Fluid Mechanics Lisbon", Portugal, pp. 07-10, 2014 July

Jones, G.G., Bouamane, L. "Historical trajectories and corporate competences in wind energy". Harvard Business School Entrepreneurial Management Working Paper. Vol. 4, No. 11-112, 2011 May.

Jan, B. "Wake Measurements Behind An Array Of Two Model Wind Turbines", KTH School of Industrial Engineering and Management Energy Technology EGI-2011-127 MSC EKV 866

Division of Heat and Power Technology SE-100 44 STOCKHOLM, October 31st, 2011.

D'Ambrosio, M., Medaglia, M. "Vertical Axis Wind Turbines: History, Technology and Applications", Master thesis in Energy Engineering, pp. 3-18, May 2010.

"Wind Turbine Blade Design Optimization, Anonymous MIT Students", Massachusetts Institute of Technology, Cambridge, MA, 02139, USA, April 2010

Mansour, K., Yahyazade, M. Effects of turbulence model in computational fluid dynamics of horizontal axis wind turbine aerodynamic. WSEAS Trans. Appl. Theory. Mech. Vol. 3, No. 6, 2011 Jul.

Wu, Y.T., Porté-Agel, F. "Atmospheric turbulence effects on wind-turbine wakes: An LES study". Energies, Vol. 5, No. 12, pp. 5340-62, 2012 Dec doi:10.3390/en5125340;2012

P. Age Krogstad, and P. Egil Eriksen, Blind test calculation of the performance and wake devel-opment for a model mind turbine. Journal of Re-newable Energy, 9 (5) (2012) 325-333.

Author information

Alireza shirzadegan: he received his Bachelor's degree in mechanical engineering frrom the University of Mashhad and he received his master's in aerospace engineering from Tarbiat Modares University and he is PhD student in the aerospace engineering from the azad Tehran University. His research interests include Fluid mechanics, aerodynamics and wind turbine.

Reza Aghaei Togh: He received his Bachelor's degree in mechanical engineering from Tabriz University and He re-ceived his master's and PhD in aerospace engineering from Amirkabir University.he is Faculty member of azad Tehran University. And Membership in some scientific journals. His research interests include Fluid mechanics, aerodynamics, wind turbine.